Journal of Materials Chemistry C

Giant Surfactants for the Construction of Automatic Liquid Crystal Alignment Layers

Journal:	*Journal of Materials Chemistry C*
Manuscript ID	TC-REV-01-2019-000422.R1
Article Type:	Review Article
Date Submitted by the Author:	19-Mar-2019

Complete List of Authors:	Yoon, Won-Jin; Chonbuk National University, Polymer-Nano Science and Technology Lee, Kyung Min; US Air Force Research Lab, ; Azimuth Corporation, Evans, Dean; Air Force Research Laboratory, Materials and Manufacturing Directorate McConney, Michael; Wright-Patterson Air Force Base, US Air Force Research Laboratory Kim, Dae-Yoon; Chonbuk National University, Polymer-Nano Science and Technology Jeong, Kwang-Un; Polymer Bin Fusion Research Center, Chonbuk National University, Department of Polymer Nano-Science and Technology

Journal Name

ARTICLE

Giant Surfactants for the Construction of Automatic Liquid Crystal Alignment Layers

00Received 00th January 20xx,
Accepted 00th January 20xx

DOI: 10.1039/x0xx00000x

www.rsc.org/

Won-Jin Yoon,[a] Kyung Min Lee,[b] Dean R. Evans,[b] Michael E. McConney,[b] Dae-Yoon Kim,*[,c] and Kwang-Un Jeong*[,a]

There has been considerable interest in nanomaterials for the development of anisotropic molecular alignment layers for electronic and biomedical applications. This review covers the recent progresses in the design, synthesis, and characterization of the automatic liquid crystal (LC) alignment layer. Amphiphilic hybrid nanomaterials consisting of organic parts and inorganic cores can interact favorably on the LC media and substrates resulting in the uniaxial orientation of LC molecules in a specific direction. Among such systems, this review emphasizes giant surfactants showing automatically self-assembled 2D monolayers. Polymerizable giant surfactants allow us to build robust molecular alignment layers via a one-bottle approach. We believe that the automatic LC alignment layer constructed by doping giant surfactants can realize practical applications in smart materials.

1. Introduction

Liquid crystal (LC) molecules are used as functional materials not only for optical displays such as lenses but also for smart devices such as micro-robots.[1-3] LC materials have been incredibly successful in the LC display (LCD) industry because of low-power consumption, thin profile, and low manufacturing cost.[4-6] LCDs have various modes which can be classified into twisted nematic (TN), vertical alignment (VA), in-plane switching (IPS), and fringe-field switching (FFS) modes depending on the LC alignment direction and the electrode configuration of the cell.[7-11] The fabrication of LC alignment layers is one of the key technologies in LC device applications. Since the LC molecules have an anisotropic shape, the anisotropic properties can be altered by the director of the molecule. Therefore, the orientation of the LC molecules having a uniaxial monodomain is important to control anisotropic physical and optical properties over a wide area.[12] The development of aligned anisotropic smart organic materials is an important technology in organic devices as well as LCDs because the physical and chemical properties are greatly influenced by the alignment of the anisotropic material.[13] For example, the molecular orientation of an actuator can control the direction and mechanical force of actuating motion.[14-18]

Homogeneous and homeotropic LC alignment is the most common and representative molecular alignment in LCD mode. In the zero-field state, the LC director in VA mode is aligned perpendicular to the substrate and the transmittance becomes dark, while the LC director is aligned in parallel to the substrate in planar

[a] Department of Polymer-Nano Science and Technology, Chonbuk National University, Jeonbuk 54896, Korea.
[b] US Air Force Research Laboratory, Wright-Patterson Air Force Base, Ohio 45433, USA.
[c] Department of Materials Science and Engineering, Massachusetts Institute of Technology, Massachusetts 02139, USA.
E-mail: kujeong@jbnu.ac.kr (K.-U. Jeong), kdaeyoon@mit.edu (D.-Y. Kim)

Won-Jin Yoon

Won-Jin Yoon received his BS degree in 2014 and MS degree in Department of Polymer Nano Science and Technology from Chonbuk National University (Korea) in 2016. He is pursuing his Ph.D degree under supervision of Prof. Kwang-Un Jeong. His research interests are focused on functional materials for alignment of liquid crystals and fabrication of optical devices.

Kyung Min Lee

Dr. Kyung Min Lee received his Ph.D. in Polymer Engineering at The University of Akron (USA) in 2002 under the guidance of Prof. Chang Dae Han. Since 2010, he has worked at the US Air Force Research Laboratory at Wright-Patterson AFB. His research interests include the development of cholesteric liquid crystal materials as electro-optic devices.

alignment (PA) mode.[4-6, 19-21] To obtain a dark state in the zero-field state, the LC director in PA mode should be parallel to the polarizer. Therefore, additional processes, such as mechanical rubbing, are required.[22-26] The LC alignment mechanism is associated with physical morphologies. Based on Berreman's elastic continuum theory, the LC molecules are aligned parallel to the microgrooves created to minimize the elastic distortion energy.[27-29] In the chemical interaction model proposed by Geary et al., the polymer side chains or their substituents of the alignment layer are aligned by the unidirectional rubbing process or by the polarized light irradiation.[23, 30-33] Over the decades, polyimide (PI) has been commonly used as PA and VA materials due to its excellent thermal and chemical stability.[34-43] Due to the mechanical rubbing process and the high temperature curing process for an extended period of time, conventional PI alignment layers are not suitable for the application of flexible and bendable displays.[44]

To replace conventional PI alignment layers[44], confined geometry[45-50], lyotropic coating[51], and photo-alignment[52-65] techniques have been developed. More recently, phase separation induced LC alignment has been studied using lecithin, silane and other nanomaterials.[68-73] Nanoparticle-induced LC alignment is very attractive due to its desirable electrical and optical properties such as low driving voltage, memory effect and frequency modulation response.[74, 75] Since most nanoparticles have strong interactions between themselves and a low compatibility with LC molecules, micrometer aggregates are formed in the LC medium causing, severe light scattering.[76-81] To overcome this drawback, substituted nanoparticles with a LC-favoring mesogenic group have been proposed.[82-84] The mesogen-modified nanoparticles act as a surfactant between the substrate and the LC medium. At optimized concentrations and temperatures, the mesogen-modified nanoparticles can migrate to the surface of the substrate to form a continuous monolayer. The formed monolayer can induce the alignment of LC molecules. Simple amphiphilic surfactants consisting of polar head groups and hydrophobic tails have also been studied for LC alignment.[85-89] Subsequent photopolymerization of the reactive mesogens can improve the chemical, mechanical and electrical stability of the LC alignment layer that is formed automatically by amphiphilic surfactants and nanoparticles.

Herein, we provide an overview of LC alignment materials based on the contributions of the pioneering researches in both fundamental principles and practical applications. Section 2 briefly reviews conventional LC alignment layers, such as polymer-based alignment layer, confined geometry, lyotropic solution coating and photo-alignment. Chemically and physically modified interfaces are critical for determining the electro-optical properties of LC devices. In Section 3, nanoparticle doping in LC systems for automatic molecular alignment is described. Section 4 describes amphiphilic surfactants for LC alignment by surface modification. Understanding interface chemistry and physics as well as intermolecular interactions is essential for controlling LC alignments. The last section details the concept of a polymer-stabilized LC alignment layer and briefly reviews its practical application. Finally, conclusions and outlooks on the topic are provided.

2. Conventional methods for LC alignment layer

Anisotropic molecules can be oriented in a uniaxial direction along a physically modified surface geometry.[45-51] In addition, the orientation characteristics of LCs strongly depend on the chemical structure of the coated material on the substrate due to the affinity difference between the molecular building blocks.[30-33] This section describes the effect of the LC alignment layer made from a rubbed surface and a patterned structure.

Dean R. Evans

Dr. Dean R. Evans received his B.S. in Physics from The Citadel (Charleston, SC) in 1992 and his M.S. and Ph.D. in Physics from the University of Georgia in 1995 and 2000. Since 2000, he has worked at the Air Force Research Laboratory, in the Materials and Manufacturing Directorate at Wright-Patterson Air Force Base. He is a Fellow of the American Physical Society, the Optical Society of America, the International Society for Optics & Photonics (SPIE), and the Air Force Research Laboratory. His research interests include photorefractive crystals, liquid crystal hybrid devices, and ferroelectric nanoparticles.

Michael E. McConney

Dr. Michael E. McConney Received his B.S.E. from the University of Iowa in 2004 in Chemical Engineering and his Ph.D. in Polymer Engineering from Georgia Institute of Technology in 2009. He has worked in the Materials and Manufacturing Directorate of Air Force Research Laboratory since 2009, where he first started as a National Research Council Postdoctoral Fellow under the advisement of Dr. Timothy Bunning. His primary research interest is in anisotropic materials, which includes liquid crystals, photorefractive crystals and composite multiferroic crystals.

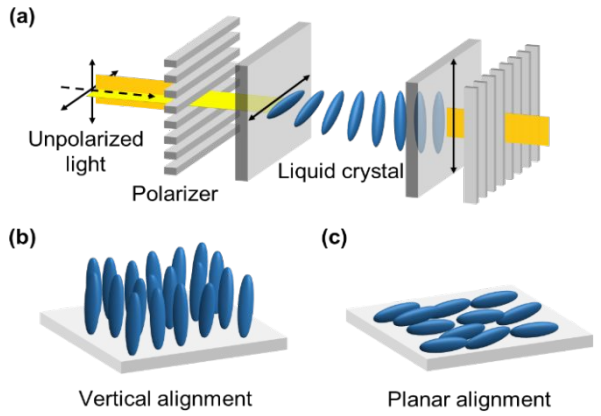

Fig. 1 Schematic illustration of (a) LCD, (b) vertical alignment and (c) planar alignment.

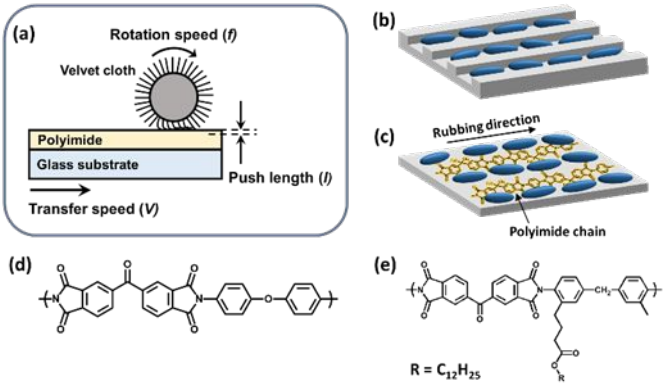

Fig. 2 Schematic image of (a) rubbing system, (b) Berreman's model of physical alignment, (c) molecular model of chemical alignment, and molecular structures of typical (d) planar alignment and (e) vertical alignment.

LCDs have been widely used from personal computers to mobile phones, televisions and automobile displays.[1-3] The LC devices consist of LC molecules sandwiched between transparent substrates with crossed polarizers and pixel electrodes.[7-11] LC molecules in LC cells are aligned by the surface anchoring force from the alignment layer. As shown in Fig. 1a, the LC molecules in LC cells can control the transmission intensity by changing the polarization direction of the light. These types of LCDs are mainly classified into VA, PA and TN modes depending on the alignment layer and the electric field application.[7-11] Since the LC molecules are aligned perpendicular to the substrate in VA mode (Fig. 1b), the VA LCD has several advantages such as a high contrast ratio and a rubbing free process.[4-6] On the contrary, the LC molecules in the PA mode are aligned parallel to the substrate (Fig. 1c).[22-26] PA LCDs exhibit good color reproduction, wide viewing angle and sunlight visibility.[34-36] This indicates that the performance and efficiency of the LCD can be manipulated by LC molecular orientation, induced by a surface alignment layer.

To fabricate an anisotropic surface for LC alignment, polymer coatings with rubbing the surface in a specific direction have been widely used.[22-26] First, the polymer solution is coated on top of the substrate using spin, dip or spray coating. The polymer coated surface is subsequently rubbed with a velvet cloth to produce an anisotropic LC alignment layer (Fig. 2a).[22] The LC alignment on the mechanically rubbed surface can be explained by Berreman's elastic continuum theory.[27-29] Microgrooves are formed along the rubbing direction. Berreman's elastic continuum theory does not take into account molecular interactions between LC molecules and coated materials; therefore, the director of the LC molecule is aligned parallel to the longitudinal direction of the microgrooves, resulting in the lowest surface energy and the most stable conformation (Fig. 2b). Numerous experimental studies have been conducted to

Dae-Yoon Kim

Dr. Dae-Yoon Kim is currently a postdoctoral associate researcher at Department of Materials Science and Engineering from Massachusetts Institute of Technology (USA). He did his doctoral work in Department of Polymer Nano Science and Technology and he received his Ph.D. degree from Chonbuk National University (Korea). He was awarded "Glenn H. Brown Prize" from International Liquid Crystal Society in 2018. His research interests focus on the nano- to macro-scale molecular assemblies for smart sensors. At present, he is working on supramolecular materials with extreme physical properties.

Kwang-Un Jeong

Dr. Kwang-Un Jeong received his B.S. in Fine Chemical Engineering from Chonnam National University (Korea) in 1998 and M.S. in Materials Science and Engineering from Gwangju Institute of Science and Technology (Korea) in 2000. After receiving his Ph.D. in Polymer Science from The University of Akron (USA) in 2005, he worked as a post-doctoral researcher for two years under supervision of Prof. Stephen Z. D. Cheng (The University of Akron) and Prof. Edwin L. Thomas (MIT). Since 2007, he has worked as a professor at the Department of Polymer-Nano Science and Technology, Chonbuk National University of Korea

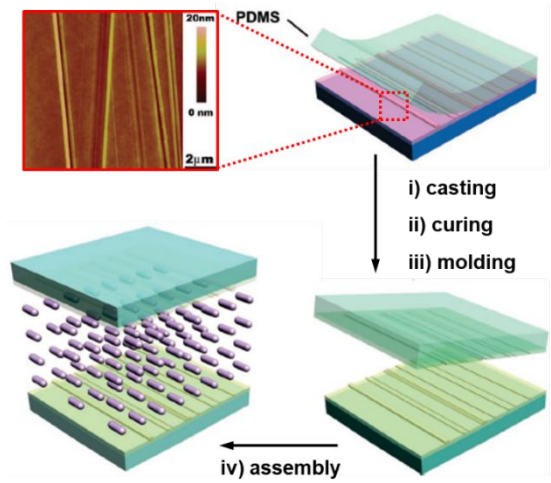

Fig. 3 Formation of the relief structures by replication and transfer method for the LC alignment layer. The inset shows the morphology of the surface of rubbed polyimide measured by AFM.

support Berreman's elastic continuum theory.[27-29, 45-50] Lin et al. presented the importance of topography for LC alignment in experiments using molecular scale nanoimprint, a replication of a rubbed polymer substrate.[50] As shown in Fig. 3, the PI solution is first spin-coated onto a silicone (Si) substrate. After curing at 250 °C, a gentle rubbing of the surface creates microgrooves along the rubbing direction. This rubbed substrate itself can induce PA of LC because of the morphological anisotropy observed by atomic force microscopy (AFM). The depth and width of the grooves are approximately 20 nm and 50 nm, respectively. To fabricate a mold for a soft template, a polydimethylsiloxane (PDMS) prepolymer is coated on the rubbed Si substrate. After curing, the formed soft template is peeled off and placed onto an indium tin oxide (ITO) coated glass. After injection of a polyurethane (PU) formulation by capillary flow, it is cured for reference group of PI alignment. The LC cell is fabricated by sandwiching the LC with the imprinted polymer films. The contrast ratio is measured by rotating the LC cell between two crossed polarizers. The maximum and minimum light transmission intensities observed at 0° and 45° indicate that the anisotropic surface morphology provides an excellent PA of LC.

However, it has been well documented for various surface molecules that induce VA of LCs that it is difficult to clearly explain the effect using Berreman's elastic continuum theory. To interpret this phenomenon, the chemical interaction between the LC

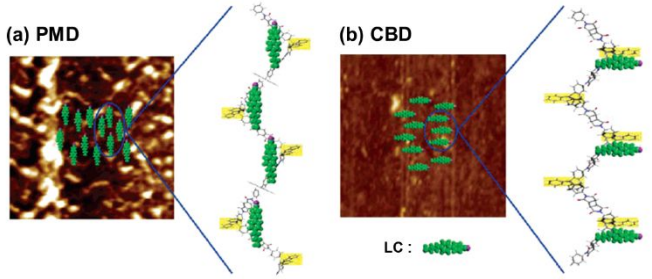

Fig. 4 Configuration model in the oriented polymer film, and the LC alignment induced by the (a) PMD and (b) CBD.

molecules and the substrate materials is introduced.[23, 30-33] Geary et al. claimed that it had a significant effect on the alignment of LC. When LC molecules are loaded onto the rubbed surface, anisotropic molecular interactions occur between the LC molecules and aligned side chains, backbones, and other substituents of the surface compounds. The initially aligned LC molecules near the surface ultimately induce bulk molecular orientation by the soft epitaxial orientation (Fig. 2c).[22] Therefore, considering topological features as well as chemical identification is a key factor in achieving molecular orientation in a particular direction.[90] Because PI exhibits excellent mechanical, thermal, and electrical properties, it has been widely used to obtain PA and VA of LCs.[34-43] Linear PIs without side chains are often used for PA of LCs (Fig. 2d).[23, 34,35] Hahm et al. studied two PIs to investigate the relationship between the chemical structure of the alignment material and the molecular orientation of LC (Fig. 4a).[91] Based on the results of Fourier-transform infrared (FTIR) experiment, it is realized that the main chains of both PIs are arranged parallel to the rubbing direction. The C-N absorption band from imide group at 1365 cm^{-1} is intense when the direction of the polarized IR beam matches the rubbing direction. The LC cell fabricated with rubbed pyromellitic dianhydride (PMD) has PA of LC molecules, which is similar to what is reported for a conventional PI anchored system used in the LCD industry. When cyclobutanyltetracarboxylic anhydride (CBD) is used as an alignment layer, the LC molecules are aligned perpendicular to rubbing direction. Even though the chemical structure between the PMD and CBD is nearly identical, a completely different LC orientation is observed due to the different chemical affinities. The phenyl ring is introduced into the backbone of CBD, but for the PMD it is the cyclobutanyl ring. Note that LC molecules show the

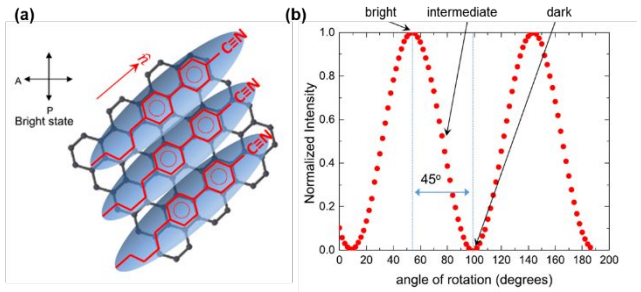

Fig. 5 (a) Schematic illustration of the alignment of the anisotropic molecules on the graphene surface. (b) The director is orientated at 45° with respect to the crossed polarizer and analyzer.

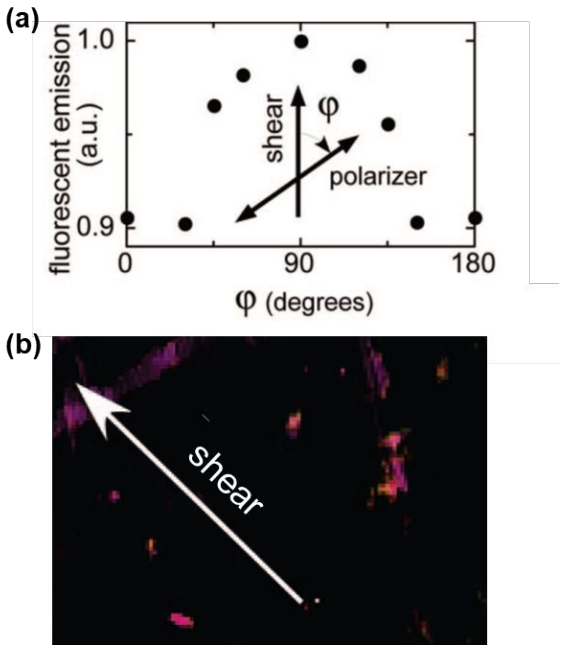

Fig. 6 (a) Intensity of emission of oriented DNA film with fluorescence dye. (b) POM image of the LC cell fabricated with the sheared DNA film.

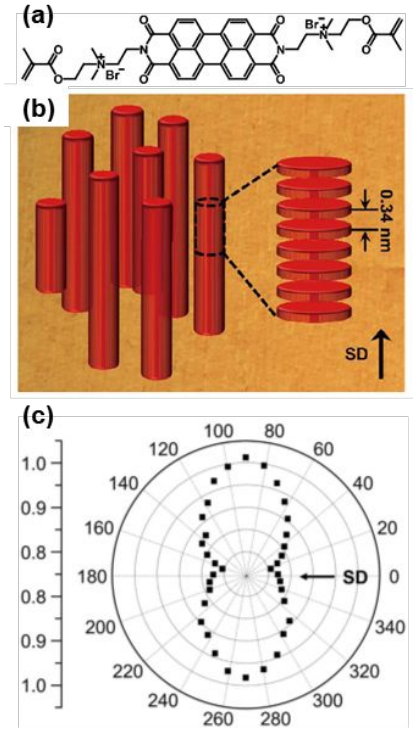

Fig. 7 (a) Chemical structure of polymerizable chromonic dye and (b) its self-assembled packing arrangement in the lyotropic mesophase, where SD is the shear direction. (c) Polarized absorption intensity of the LC cell rotating the optic axis of polarizer. Here, the significant absorption band corresponding to the vibration of cyanide group in the LC molecule is selectively detected at 2225 cm^{-1}

favorable alignment through anisotropic interactions with aromatic rings. Taken together, these results indicate that the LC alignment is determined by the play-off between the oriented segments of the main chains and the microgrooves. In general, the linear PI modified with aliphatic side chains is applied for the VA mode, which provides the pretilt angle of LC (Fig. 2e). Various PIs have been developed by slightly modifying the chemical structure to control the pretilt angle of the VA mode for achieving a faster response time, a wider viewing angle, and a higher contrast ratio.

The LC alignment induced by chemical components is further supported by the directional interaction model proposed by Stöhr et al.[90] Previous studies have shown an interesting alignment of nematic and smectic LCs explained by π-π electron stacking anchoring.[23] Additionally, the molecular orientation order of the LC molecules can be stabilized on a honeycomb lattice such as graphene, graphite, and carbon nanotubes with a binding energy of -2 eV.[92] LC cells coated with monolayer graphene can be used as LC alignment layers as well as transparent electrodes. Chemical vapor deposition (CVD) graphene grown on a copper (Cu) film can be transferred onto a glass substrate using a polymethyl methacrylate (PMMA) assisted method.[93, 94] Based on normalized intensity observation as a function of the relative rotational angle under the crossed polarizers, the LC can achieve a uniform PA state over a large-scale dimension on graphene (Fig. 5a). When the LC director becomes parallel to the polarizer or analyzer, the LC cell clearly exhibits a uniform dark state, resulting in the minimum light transmittance. The change in transmission intensity from dark to bright at every 45° rotation confirms that graphene imposes the PA on the nematic phase (Fig. 5b). Additionally, the graphene alignment layer can work as an electrode. In a uniform and parallel plate configuration, the director of LC with a positive dielectric anisotropy (+$\Delta\varepsilon$) is aligned parallel to the applied electric field (E), which is higher than the threshold voltage. Replacing the PI alignment layer with graphene can reduce the thickness of the overall optical element, thus minimizing the transmission loss for backlit LCDs.[92] Minimizing transmission losses is especially critical to emerging technolongies, such as the use swichable LC diffractive waveplates for many applications including multi-state switchable lenses, virtual reality displays, and beam-steering that is being developed to enable self-driving cars. These devices are achieving their unique properties by stacking many LC devices to achieve many states and thus the minimizing the transmission losses of each layers is critical because the losses are compounded by their inherently stacked architecture.[95]

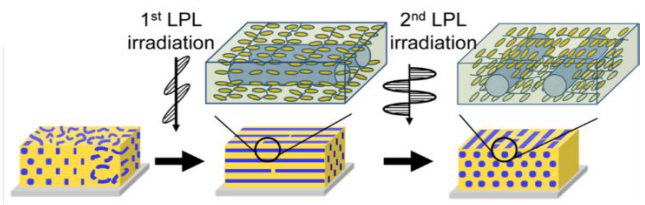

Fig. 8 Photoalignment procedures using the azobenzene based polymers. After uniformly coated (left) on the substrate, the film is aligned (middle) by LPL irradiation, and then it can be subsequently realigned by LPL (right) in the orthogonal direction.

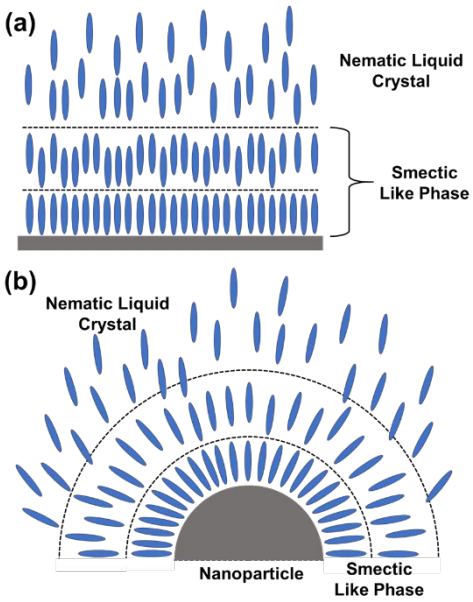

Fig 9. Schematic images of smectic like phase and alignment of LC directors on (a) flat surface and (b) spherical nanoparticle.

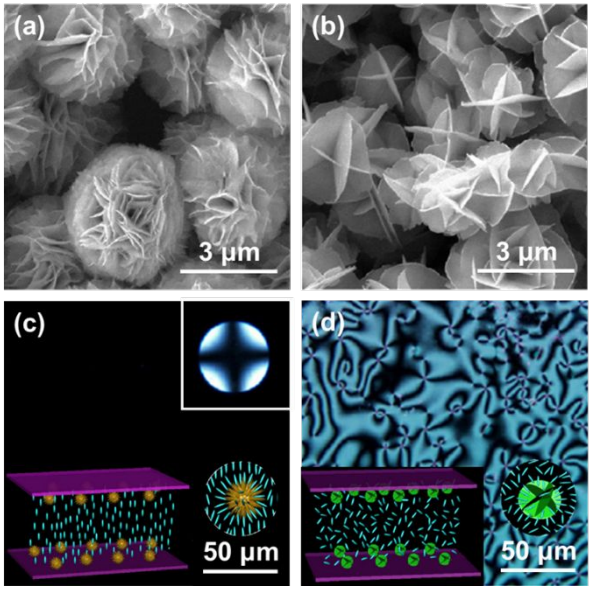

Fig. 10 SEM images of (a) flower-like and (b) frame CuS nanoparticles. POM images of LC cell doped with (c) 0.05 wt% flower-like CuS and (d) 0.05 wt% frame CuS. The inset of Fig. 10c and 10d represent schematic illustration of molecular orientation, respectively.

From a processing perspective, the lyotropic LC (LLC) has received considerable attention both in academic and industrial contexts. The LLC molecule has an amphiphilic structure. They can commonly be self-assembled in polar solution to form micelles, vesicles, microtubules, and fibrillar superstructures, and they show excellent processability.[96-99] DNA nucleotides and amphiphilic chromogens can form nematic and columnar mesophases depending on their concentration. After applying mechanical shear at a constant rate, a well-oriented LLC film can be obtained through the evaporation process.[100] Uniaxially oriented LLC films have been used as alignment layers for LC materials due to their high regularity. As shown in Fig. 6a, sheared dehydrate films with DNA and dye show maximum fluorescence at 90°, indicating that the DNA strands are aligned in the shear direction.[101] To verify the effect of the oriented DNA layer on the LC alignment, anisotropic LC molecules are introduced at its isotropic phase temperature. The lowest transmittance is measured at $\theta = 40° + 90° \times n$ as expected in polarized optical microscope (POM) images (Fig. 6b). This is because the LC molecule interacts with polar grooves made of the phosphate chains of DNA. The predetermined polar angle of the LC molecules from the alignment layer influences the electro-optical performance including the driving voltage, the response time, and the viewing angle.[101,102] However, the practical application of conventional LLCs as molecular alignment layers is limited due to the intrinsic fluidity and the lack of mechanical stability.[96-101]

Recently, cross-linkable groups have been incorporated into LLC molecules to meet the requirements for high-performance sophisticated materials.[97,98] Polymerization of lyotropic LLC film shows promising stability for a wide range of chemical and physical properties. Lim et al. synthesized a perylene-based reactive mesogen (PBRM).[51] The PBRM molecule is obtained by the imidation reaction of amine with anhydride. The aromatic core of perylene induces strong intermolecular face-to-face interaction. Charged amine-bromine ionic groups at both ends of the molecule improves solubility in aqueous solution (Fig. 7a). When the ionic interaction is balanced with the π-π interaction, the LLC molecules are self-assembled into a nanocolumn. Methacrylate functional groups can fix an ordered phase through the polymerization process. At a concentration of 10 wt% to 30 wt%, the aqueous PBRM solution exhibits a typical columnar nematic phase at room temperature. The uniaxially oriented PBRM film possesses the E-type optical property showing that an extraordinary ray is transmitted and an ordinary ray is absorbed corresponding to the shear direction (SD). As can be seen in Fig. 7b, the self-assembled nanocolumns are aligned in parallel to the SD (Fig. 7b). Macroscopic defects are not found after photo-polymerization, indicating that the ordered molecular arrangements are well maintained. When LC molecules are injected into the LC cell assembled in an antiparallel direction, the LC molecules are aligned perpendicular to the SD of the PBRM (Fig. 7c). Note that the orientation of LC can be controlled by the anisotropic surface of the alignment layer. The polarity of the PBRM is very high due to the cationic charge in the molecule and the PBRM polymer chains are aligned parallel to the self-assembled nanocolumn direction; therefore, the polar groups of the PBRM are oriented alog perpendicular to the nanocolumn direction. The molecular interaction between the polar group of the PBRM and the cyanide groups of the LC molecule induces a uniaxial orientation and results in a small pretilt angle close to zero. Based on these results, it is known that a molecular interaction on the surface is important for the LC alignment on LLC films.

An important feature for aligning LC molecules on conventional systems is the anisotropic surface energy originating from mechanically rubbed surface topography or anisotropically aligned molecules.[22-26, 34-36] However, the mechanical rubbing process causes serious problems including static electricity and macroscopic defects which can damage the thin film transistor (TFT) of the

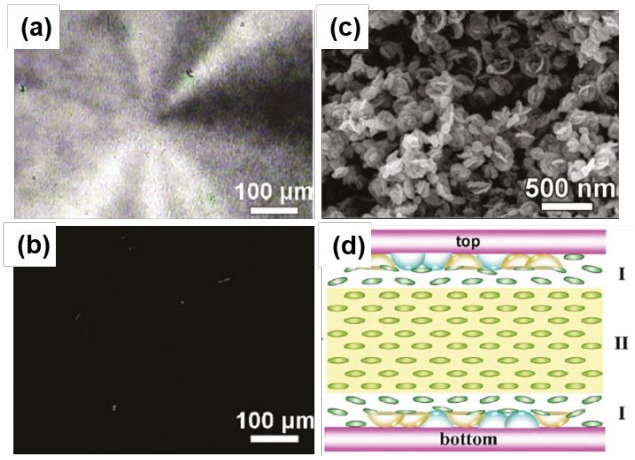

Fig. 11 POM images of 0.01 wt% Ni bowl doped LC cell in (a) bright field and (b) dark field. (c) SEM image of Ni bowls. (d) Schematic illustration of the PA of the LC.

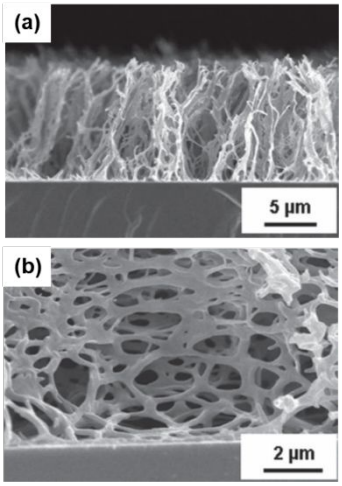

Fig. 12 SEM images of (a) the VA and (b) PA oriented polymer network.

LCD.[45] A photoalignment of LC molecules is one of the good alternatives to overcome the major drawbacks of mechanical contact processes.[54-65] Since the report from Gibbons et al., there has been many studies on the photoalignment of LCs for commercialization.[61] Photochemical reactions can control the alignment of LCs by irradiating the coated materials containing photochromic mesogenic functions. Schadt et al. use poly(vinyl cinnamate) to achieve the orientation of LCs, but fail to commercialize this due to image sticking problems.[103] When a uniformly coated azobenzene-based polymer on a substrate is exposed to linearly polarized light (LPL), the LC favored mesogenic part can be aligned normal to the polarization direction. In-plane or out-of-plane alignment depends on the *trans-cis* isomerization (Fig. 8). Since the LC molecules preferentially interact with the *trans*-azobenzene owing to their rod-like geometry, the LC molecules are aligned parallel to the direction of the *trans*-azobenzene molecule. As a non-contact method, the photoalignment layers are also useful to align other functional materials such as dichroic dyes, electroluminescent and conductive materials.

3. Nanoparticle-induced automatic LC alignment

This section describes nanoparticle-induced LC alignment, which represents automatic LC alignment. As mentioned above, conventional LC alignment requires a two-step process of pretreatment of the substrate and subsequent LC loading.[34-44] Although the photoalignment of the LC is a noncontact method, a two-step process is still required for the alignment layer and LC injection.[54-65] Recently, a one-step process using nanoparticles without additional pretreatment has attracted for the LC alignment.[68-84] Nanoparticles dispersed in the LC matrix act as defects that interfere with the self-assembly of LC molecules. In the case of LC molecules exhibiting the nematic order, the phase around nanoparticles is changed into a smectic-like as phase previously proposed by de Gennes (Fig. 9).[104,105] The smectic layer which has an equivalent average molecular length is formed on the surface of nanoparticles by strong molecular anchoring energy. The smectic-like phase is considered in the twist and bend elastic constants of LC near a particular surface. The smectic-like phase near the nanoparticles can be reoriented to the normal direction of the nanoparticle surface, and then the LC molecules forming the layer next to the smectic layer can also be rearranged in the bulk. This phenomenon is due to topological defects of the surface and the difference in free energy between the LC and the surface. According to the semi-empirical Friedel-Creagh-Kmetz (FCK) rule, if the surface energy of the substrate is greater than the surface tension of the LC, the LC is planarly aligned, and when reversed, the LC is vertically aligned.[105] Therefore, the nanoparticle doping process is one of the fascinating candidates to control the surface topology by forming a self-assembled monolayer (SAM).

Recently, many types of nanoparticles such as a polyhedral oligomeric silsesquioxane (POSS)[72-74, 79-81], fullerene (C_{60})[82] and metallic particles[75-78] have been used to achieve PA and VA of LC. These nanoparticles are directly doped into the LC media, and the concentration of the nanoparticles is optimized for complete LC alignment across the entire area. The doped nanoparticles can initially migrate on the substrate surface. The nanoparticle SAM on the substrate reduces the surface energy and ultimately induces uniaxially oriented LC. Liu et al. synthesized copper sulfide (CuS)-based nanoparticles with two types of hierarchical nanostructures.[107] As shown in Fig. 10a and 10b, scanning electron microscopy (SEM) images show that the average diameter of the flower-like and the frame-like CuS is 4 μm, and 3 μm, respectively. Flower-like CuS is the result of regular self-assembly of the nanosheets, while frame-like CuS is obtained by the agglomeration of sparse nanosheets. CuS is dispersed into the LC medium to explore the LC alignment by nanoparticle SAM morphology. Without CuS, a Schlieren texture is observed, indicating that the director of each LC domain is disorderly arranged. When the concentration of flower-like CuS is adjusted to 0.01 wt%, the dark phase is emerged, suggesting the partial VA of LC molecules. As the concentration of flower-like CuS increases from 0.01 wt% to 0.05 wt%, a perfect VA of LC is observed, as shown in Fig. 10c. The

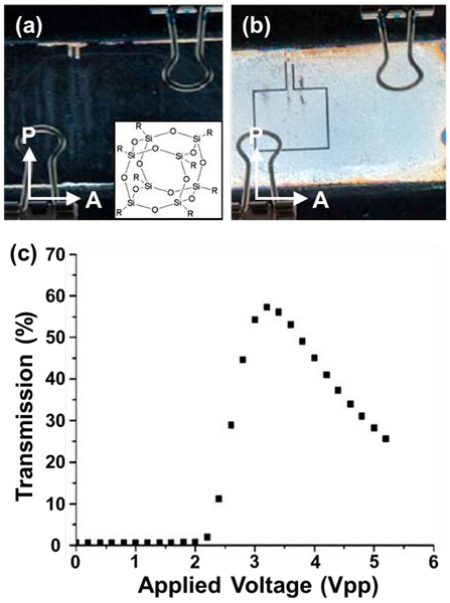

Fig. 13 POSS-induced VA in the LC cell viewed under crossed polarizers (a) without an *E* field, and (b) with an applied *E* field, and (c) its voltage-dependent transmission spectra.

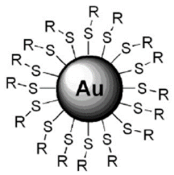

Au NP —R	size distribution ± SD (nm)
$AuAT_6$ $-C_6H_{13}$	1.58 ± 0.44
$AuAT_{12}$ $-C_{12}H_{25}$	5.41 ± 0.93

Fig. 14 Schematic of alkyl thiolate capped nanoparticles for the VA of the LC.

uniform dark image demonstrates that the performance of the LC alignment is gradually enhanced by the amount of flower-like CuS. For comparison, 0.05 wt% of the frame-like CuS is also doped into the LC medium, but only the Schlieren texture is observed (Fig. 10d). This result demonstrates that doping frame-like CuS does not help to align the LC in a certain direction. A mechanism has been proposed to explain the VA of LC induced by flower-like CuS. First, flower-like CuS doped in the LC medium is adsorbed on the inner substrate to reduce the surface defect. Second, the CuS forms the SAM that maintains the system at the lowest energy state. Finally, the LC molecules tend to be inserted into the holes and are arranged according to the growth direction around the flower-like CuS. The nanosheets grow perpendicular to the substrate, and produce a strong anchoring force in the VA direction of the neighboring LC. However, the frame-like CuS is difficult to form the VA of LCs because the nanosheets of the framework are large and are located in all directions.

Because nanoparticles including gold (Au) and cadmium selenide (CdSe) are simple spheres without complex structures of several nanometers, doping nanoparticles in most LC system induce VA rather than PA.[76-78] On the other hand, Zhou et al. has developed nickel (Ni) nanoparticles that induce PA of LC.[108] SEM images of prepared bowl-like Ni nanoparticles show a diameter of 250 nm and a shell thickness of 10 nm (Fig. 11c). Rotating the LC cell doped with 0.01 wt% Ni bowls at 45° produces a uniform dark phase (Fig. 11b), indicating that PA of LC is abstained with good birefringent change (Fig. 11a). Fig. 11d represents the molecular arrangement of the LC composite. The Ni nanoparticles are adsorbed on both sides of LC cell and self-assembled into the 1D structure and arranged along the filling direction due to the fluid effect. As illustrated in zone I, the LC molecules close to the 1D ordered Ni bowls are aligned parallel to the surface. The aligned LC molecules then induce the neighboring LC molecules in the same direction in zone II.

To confirm the nanoparticle-induced LC alignment, a reactive mesogen (RM) composed of a rigid mesogenic moiety, a polymerizable acrylate group and a flexible alkyl spacer between the core and the end group is often used. The RM can be effectively oriented along the molecular orientational order of the LC. Zhao et al. used both Ni nanospheres and nanobowls to induce VA and PA of LCs.[109] At first, the optical cell is filled with a homogeneous mixture of nematic LC, RM, Ni nanoparticles and photo-initiator. After a few minutes, the LC molecules are uniformly aligned in the uniaxial direction. UV light is then used to irradiate the optical cell to induce the *in situ* photo-polymerization of the RM. The RM dissolved in the LC medium forms a cross-linked anisotropic polymer network. This approach provides a permanent anisotropic orientation. After UV curing, the optical cell is carefully opened and the cured LC film is rinsed with cyclohexane to remove any unreacted compounds. The SEM image show a uniform polymer network according to the LC coverage of the Ni nanoparticle layers. As shown in Fig. 12a, the cross-sectional image of the fractured optical cell exhibits the fibrous morphology oriented perpendicular to the film thickness direction. Therefore, the VA of the host LC medium induced by Ni nanospheres is successfully transferred to the polymer template. The SEM image for fractured surface fabricated with Ni nanobowls is shown in Fig. 12b, showing that the fibrous morphology is aligned parallel to the substrate. Therefore, it is visualized that the LC molecules are aligned parallel to the substrate.

Using phenethyl-substituted polyhedral oligomeric silsesquioxane (POSS) as a nanoparticle dopant that can be mixed

directly with the LC medium, POSS-induced VA of LC is reported by Jeng et al.[73] The VA of LCs by POSS is much easier than conventional chemical synthetic methods. In the LC medium, a few wt% of POSS is dispersed in the acetone solvent by an ultrasonic mixer. After evaporation of the volatile solvent, the POSS-doped LC mixture is loaded into an LC cell with a cell gap of 6.2 μm. The LC cell viewed under the crossed polarizers shows the VA of LCs (Fig. 13a). The pretilt angle of LC is measured as 88.5°. When the applied electric field is higher than the threshold voltage, the optical transition of the LC cell changes to a white state (Fig. 13b). The electro-optical properties of the POSS-induced VA LC cell are very similar to conventional alignment layer systems. The threshold voltage recorded at 2.1 V_{pp} is similar to the value to the PI-based VA LCs (Fig. 13c). This result indicates that the addition of a small amount of POSS does not significantly affect the dielectric anisotropy and elastic constant of the LC layers. However, the response time is somewhat decreased as expected because there is no preferred orientation often generated by the rubbing process.

4. Surfactant for automatic LC alignment

Although the automatic molecular alignment achieved by doping nanoparticles is an important step in manufacturing cost, there are critical obstacles to overcome.[68-84] In the LC medium, nanoparticles form micrometer-sized aggregates by stronger nanoparticle interactions than the interactions between nanoparticles and LC molecules.[76-81] The nanoparticle aggregates formed in the LC cell are difficult to disperse into the LC media, resulting in severe light scattering and slow electrical response. To overcome these problems, functionalized nanoparticles, referred to as organic-inorganic hybrid materials, have been developed. Qi et al. demonstrated that alkylthiol-capped Au nanoparticles can alter the LC alignment (Fig. 14).[83] Two different hybrid materials are prepared by varying the length of the alkyl thiolate (C_6H_{13}, AT_6 and $C_{12}H_{25}$, AT_{12}). The size of $AuAT_6$ and $AuAT_{12}$ is 1.5 nm and 5.4 nm, respectively. VA of LCs is observed at 2 wt% of $AuAT_6$. $AuAT_{12}$, a larger size nanoparticle, requires a higher concentration (10 wt%) for the VA of LCs, but it is more compatible with LC molecules due to the large number of flexible aliphatic chains. The LC alignment is governed by the different solubility of the initially doped nanoparticles in the LC medium, and the functional groups on the nanoparticle are randomly distributed. Therefore, nanoparticles whose structure and morphology are not well defined cannot control the direction of LC alignment.

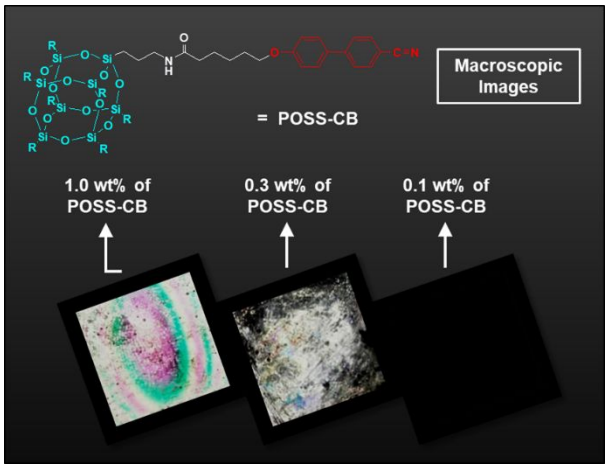

Fig. 15 POSS-based asymmetric hybrid giant surfactant and its LC alignment property in the optical cell.

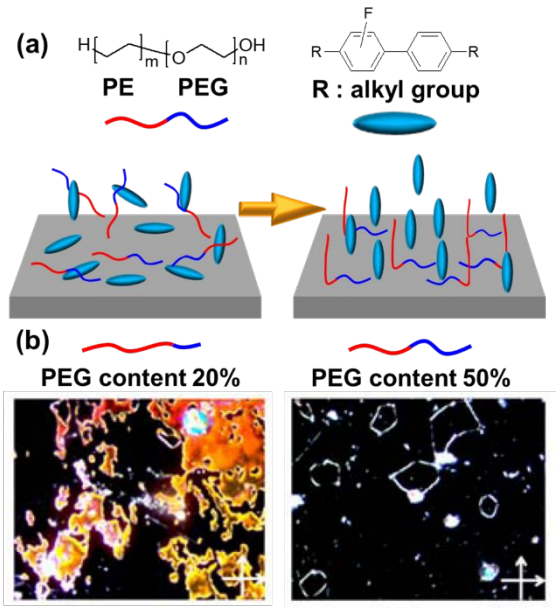

Fig. 17 (a) Schematic illustrations and molecular structure of the substrates of the LC test cell doped amphiphilic block copolymers. (b) POM images of the LC test cells containing the various concentration of the BCPP.

Site-selective functionalization of nanoparticles is very useful for controlling the self-assembly of nanoparticles on the surface, which in turn allows for tuning the automatic LC alignment. Therefore, it is necessary to precisely introduce chemical functions selectively onto nanoparticles through suitable chemical modifications. Kim et al. proposed a mono-functionalized POSS nanoparticle as an asymmetric hybrid giant surfactant.[84] The mono-functionalized POSS nanoparticles are designed to enhance intermolecular interaction between POSS nanoparticles and LC molecules as well as between POSS nanoparticles and substrates. They act as giant amphiphiles to prevent aggregation with themselves and control LC alignment. Basically, these giant surfactants consist of two different segments: the LC repel and the LC favor group. As shown in Fig. 15, POSS-CB has inorganic head group and an organic side pendant. The POSS part, consisting of silicon and oxygen, can interact preferentially with the glass substrate, but the organic side pendant can interact with the LC molecule. The degree of LC alignment is mainly affected by the amount of POSS-CB in the LC medium. The addition of POSS-CB less than 0.1 wt% readily induces the dark state of LC cell indicating a VA. By considering the calculated POSS-CB geometry with a height of 3 nm and a width of 1 nm, 0.02 wt% POSS-CB in the LC mixture can form a SAM in the entire surface of the optical cell. The inorganic POSS part constructs the two dimensional (2D) self-assembled crystalline platform on the substrate. Then, the LC molecules crawl into the empty spaces among the cyanobiphenyl tethered groups. The increased intermolecular interactions between giant surfactants and solid substrates as well as between giant surfactants and LC molecules are basically achieved by precise chemical modification of the nanoparticles.

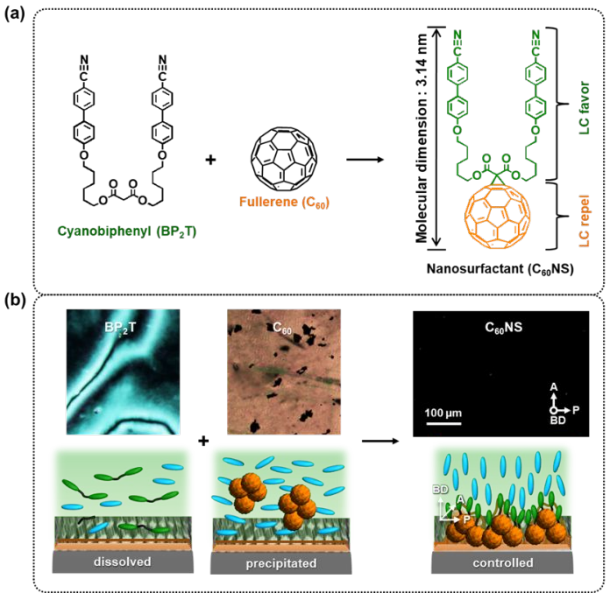

Fig. 16 (a) Chemical building blocks of $C_{60}NS$. (b) POM images of BP_2T, C_{60}, and $C_{60}NS$ doped LC cells and their corresponding molecular alignment mechanism.

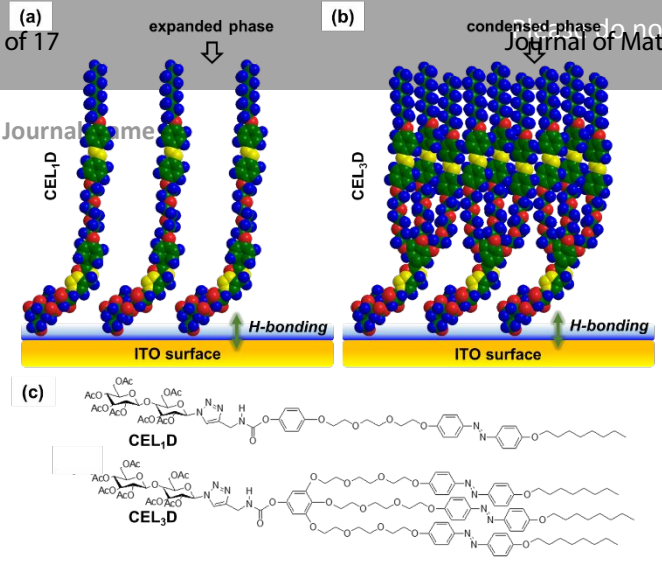

Fig. 18 Illustration of the test cell substrate prepared with (a) CEL_1D and (b) CEL_3D, and (c) chemical structures of CEL_1D and CEL_3D

With well-defined molecular structure and specific symmetry, C_{60} is another fascinating class of nanoparticle for automatic LC alignment. In particular, the mono-functionalized C_{60} can be synthesized via stoichiometry-controlled Retro-Prato and Bingel-Hirsch reactions. Kim et al. introduced C_{60}NS giant surfactant by attaching the cyanobiphenyl mesogens and the alkyl chains to C_{60} (Fig. 16a).[82] As with surfactants, it is possible to effectively bridge the solid substrates and LC molecules. To identify the key factors of each chemical building block for LC alignment, LC mixtures with C_{60}, BP_2T, and C_{60}NS are prepared, respectively, and filled into the optical cell (Fig. 16b). For C_{60} and CB_2 doped LC cells, there is no alignment of the LC in the macroscopic region. BP_2T is completely soluble in the LC medium due to similarity of the chemical structure. C_{60} nanoparticles in the LC medium precipitate immediately and do not form a SAM. LC favoring (BP_2T) and repelling (C_{60}) moieties cannot modify the surface anchoring

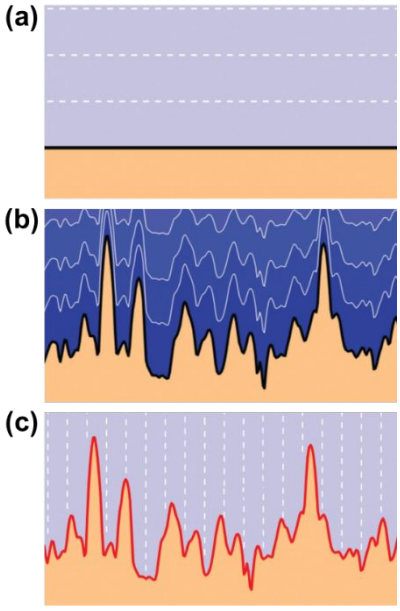

Fig. 19 Graphical illustration of modified surface morphology for the LC alignment with different roughness: (a) PA on a smooth surface, (b) PA with a high elastic distortion, and (c) VA on a rough surface.

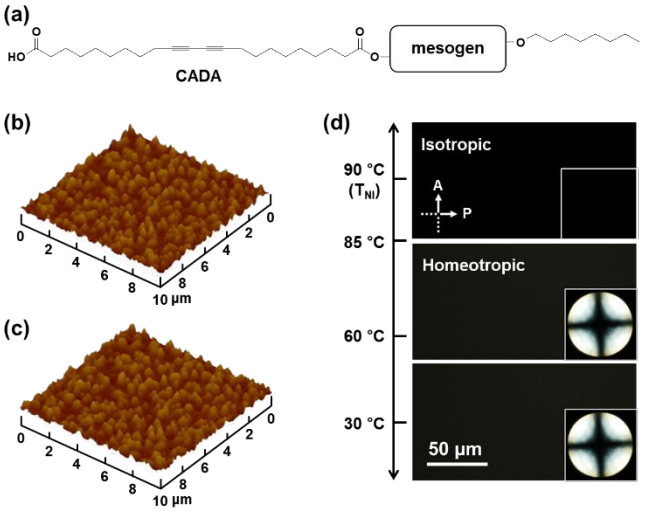

Fig. 20 (a) Chemical structure of polymerizable amphiphilic surfactant for automatic LC alignment. AFM morphology of the SAM of CADA (b) before and (c) after polymerization. (d) POM images of the 0.1 wt% CADA coated VA LC cell at various temperatures.

condition to obtain an automatic VA of LCs. In addition, other commercially available C_{60} derivatives such as [6,6]-Phenyl C_{61} butyric acid methyl ester and C_{60} pyrrolidine tris-acid also show only randomly arranged LC due to its segregation. On the other hand, the addition of C_{60}NS results in the VA of LC molecules by the automatic construction of the SAM. When 0.1 wt% C_{60}NS is doped into the LC medium, the complete dark state is detected by orthoscopic POM images. The main driving force for self-assembly is

the nano-segregation of structural motifs. The C_{60}NS itself forms a bilayer structure constructed by lateral molecular packing. If the concentration of C_{60}NS in the LC medium is high, the lamellar structure is formed before the phase-separation. Therefore, the content of C_{60}NS is optimized for VA of LC by constructing SAM on the surface.

Molecules showing the amphiphilic nature are also known to be effective materials for the automatic LC alignment layers. Since the amphiphilic molecules consist of hydrophobic and hydrophilic groups, the former part interacts with the LC molecules while the latter part has a high affinity for the ITO substrate.[85-89] Son et al. developed a block copolymer (BCPP) by chemically linking polyethylene glycol (PEG) and polyethylene (PE).[85] To investigate the effect of chain length and block copolymer concentration on LC alignment, the PE and PEG content is controlled to 20:80 to 50:50. The content of BCPP in the LC medium is optimized to 0.1 wt%. As shown in Fig. 17a, LC cells fabricated with the shorter PEG of BCPP exhibit a random texture in regions larger than the longer PEG. BCPP with a short PEG block shows lower anchoring energy to the substrate resulting in unstable LC alignment. The dark state for PEG content of 50% (Fig. 17b) indicates that the LC is vertically aligned. The increased content of hydrophilic part in the block copolymer provides sufficient affinity to adsorb onto the ITO substrate owing to its high affinity. The PE block then aligns the LCs vertically to the surface by van der Waals interaction.

For the control of LC alignment, amphiphilic supramolecules composed of dendritic building blocks can be used to form SAMs on the surface. Kim et al. synthesized a series of carbohydrate-based amphiphilic surfactants for an automatic VA layer of the LCs.[86] Utilizing the copper(I)-catalyzed cycloaddition reaction, the dendritic alkyne derivatives are click-coupled with a cellobiosyl azide compound. Depending on the number (n) of mesogenic units, the amphiphilic surfactants are abbreviated as CEL_nD (Figure 18c). The self-organization of the CEL_nD molecules by strong hydrogen bonding between the carbohydrate groups and the solid substrates can form the SAM. The tail groups determine the interaction parameters with the LC molecules. When 0.1 wt% of CEL_1D is doped into the LC cell, VA of LC is achieved. Conversely, CEL_3D does not induce VA, but PA of the LCs is achieved. Based on the AFM images of the CEL_nD, the SAM formed on the ITO surface exhibits many

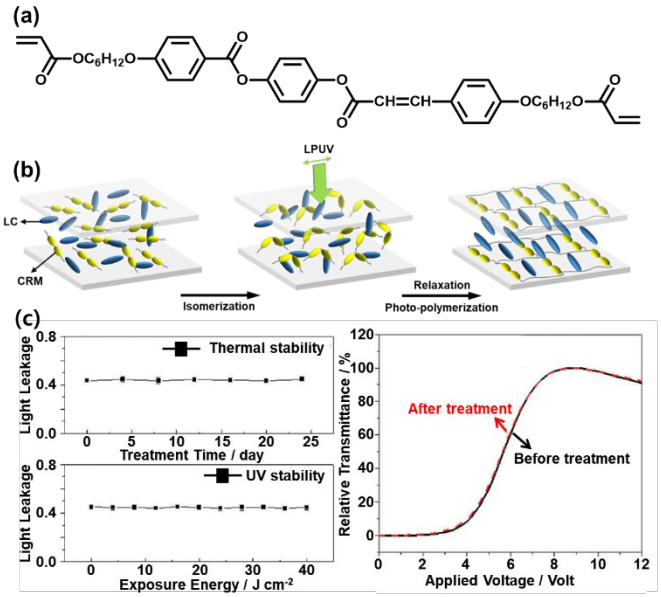

Fig. 21 (a) Chemical structure of CRM. (b) Fabrication procedure by using the photoisomerization and subsequent photopolymerization of CRM for the LC robust alignment layer. (C) UV and thermal stability test of the LC cell with PA.

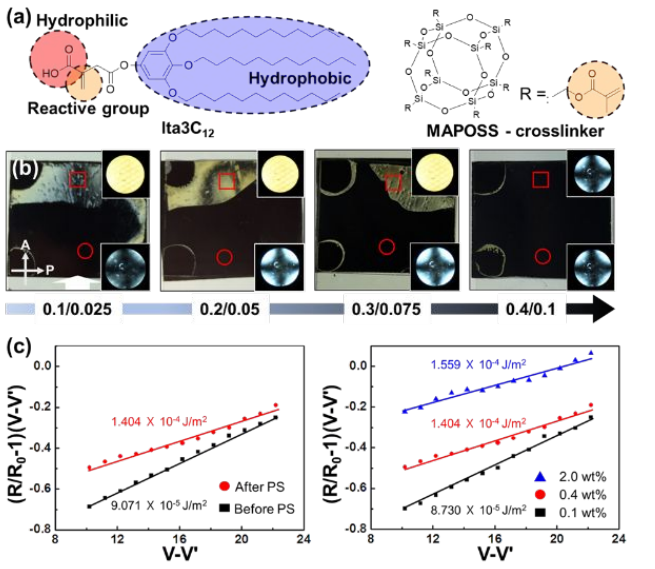

Fig. 22 (a) Molecular structure of $Ita3C_{12}$ and MAPOSS. (b) Orthoscopic POM images and conoscopic images (inset) of the LC test cell with different $Ita3C_{12}$/MAPOSS wt% ratio ranging from 0.1/0.025 to 0.4/0.1. (c) The slope of the graph corresponding to anchoring energies of before and after the polymerized LC test cells for various concentrations.

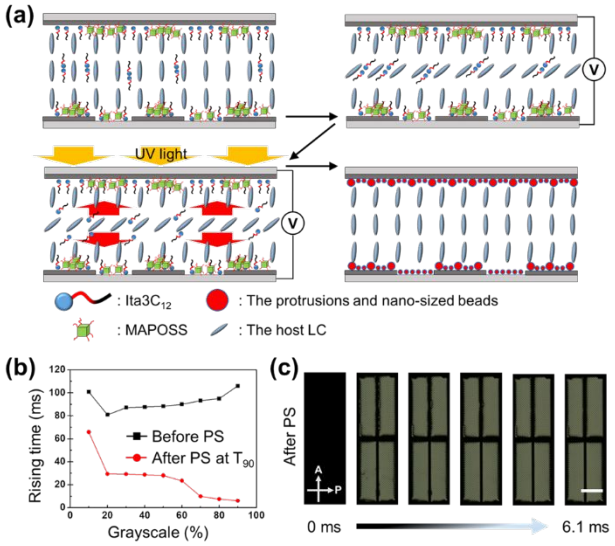

Fig. 23 (a) Schematic illustrations of the fabrication process for inducing a pre-tilt angle of the LC medium in the LC test cell. (b) Rise time vs grayscale for the LC test cell before and after polymer-stabilization (PS). (c) The time-resolved LC textures at 5.6 V after polymer-stabilization, where the white scale bars correspond to 100 µm.

protrusions and continuous uniform layers. The average height of the protrusions of CEL_nD is 4.3 nm. This result indicates that there is no topographical difference between CEL_1D and CEL_1D layers. Since the calculated length along the long axis of the CEL_nD is about 4.8 nm, it can be understood that the surfactants are deposited normal to the surface and laterally self-assembled to the monolayers. As schematically described in Fig. 18a, the CEL_1D can form the expanded structure on the surface. The LC molecules in the medium can migrate to the pore region of the expanded CEL_1D structures for the formation of VA. However, the condensed structure is constructed on the surface for CEL_3D. Even though the CEL_3D is arranged normal to the surface, the CEL_3D induces PA of LC, indicating that the LC alignment is closely related to the protrusion morphology as well as the chemical compositions (Fig. 18b). LC molecules are difficult to crawl into the condensed CEL_3D structure, rather they lie down to form PA.

One bottle approach is also proposed by Kundu et al. for the formation of VA.[110] By using azo-based dye dopants added to the LC host, VA is achieved without any pretreatment of substrates. The optical cell loaded with dye and LC mixture exhibits an initial random PA, but subsequent UV light irradiation results in VA of the LCs. In the *trans*-state, the dye molecules are dissolved in the LC host and the surface morphology does not change (Fig. 19a). When UV light is irradiated, the surface morphology changes due to a square crystalline assembly of dye molecules on a continuous layer of themselves. As a result of the increased dipole moment of *cis*-state owing to the broken symmetry, the dye molecules are phase separated from the LC molecules and closely packed together. The formation of a rough surface causes high elastic distortion of anisotropic molecules. Fig. 19b presents the cross-sectional profile of the *cis*-isomerized dye deposited surface. The light blue region represents the minimum elastic energy and the dark region corresponds to the high distortion energy. To avoid highly distorted states from dye-aggregated rough surfaces, LC molecules begin to align vertically to minimize the elastic distortion of the system (Fig. 19c).

5. Polymer-stabilized LC alignment layers

The automatic LC alignment achieved by doping the nanoparticles and surfactants can simplify the complicate multiple step fabrication process of conventional alignment layers. However, LC alignment layers composed of the SAMs formed by these low molecular weight molecules generally exhibit structural instability due to molecular exchange and rearrangement that afflicts this class of materials.[74-79] Because there is no covalent bonding or cross-linking, the organic-inorganic hybrid materials and amphiphilic giant surfactants for LC alignment lack thermal, mechanical and long-term stability. To improve the stability of LC cells, photopolymerization of anisotropic alignment systems is employed to obtain a robust SAM.[87-89, 111] Since the cross-linked structure of polydiacetylene is formed by irradiating UV light without chemical initiator, the stability of LC alignment can be secured by introducing a diacetylene moiety into the amphiphilic surfactants.[87] The carboxylic acid is located at the end of the CADA as a head group (Fig. 20a), and the CADA can induce an automatic 2D monolayer on the solid substrate. 0.1 wt% of the CADA is phase separated from the LC host and diffused onto the substrate for the formation of the VA layer. The monolayered protrusions formed by the lateral self-assembly of the CADA amphiphiles provide enough space for LC molecules to crawl into the empty spaces (Fig. 20b). Polymer-stabilized CADA LC cell also shows the VA state. In addition, the morphology of the self-assembled CADA film after polymerization is almost the same as that of the unpolymerized monolayer (Fig. 20c). This result indicates that photopolymerization of the diacetylene moiety in the SAM does not disturb the self-assembly features for LC alignment. Without photopolymerization, VA is only achieved by a slow cooling rate. However, the polymerized VA layer is independent of the cooling rate. Fig. 20d shows that the Maltese cross pattern is retained strongly at high temperatures. The crosslinked SAM of CADA is stable enough to overcome severe thermal fluctuations.

The quality and reliability of LCD depend not only on the response time, but also on the durability of the LC cell. In particular, UV and heat stability are crucial factors for the photo-induced LC alignment, because the photo-isomerization rate depends on the light exposure and the temperature change. To achieve high image quality, He et al. synthesised a photosensitive cinnamate compound (CRM) in the core containing the reactive mesogen moiety at both ends (Fig. 21a).[110] When the LC cell is exposed with the linearly polarized UV at 95 °C, the *cis*-form of CRM is converted to the *trans*-form by thermal relaxation. The molecular axis of CRM is reoriented perpendicular to the incident light; therefore, the LC molecules are also oriented perpendicular to the electric vector of the incident linearly polarized UV light. Photopolymerization forms an

anisotropic network layer and fixes the PA of the LC host (Fig. 21b). The voltage-transmittance curve of the CRM optical cell is measured after the photopolymerization to verify the stability. As shown in Fig. 21c, there is no substantial change in the electro-optical property even after the harsh UV and thermal treatment. The light leakage test further supports the stability of the PA layer. These results indicate that the automatic LC alignment and subsequent polymer stabilization processes provide sufficient stability of the LC cell.

To form an automatic VA layer, Yoon et al. proposed a photopolymerizable reactive amphiphilic surfactant ($Ita3C_{12}$) containing three dodecyl alkyl chains and a hydrophilic carboxylic acid (Fig. 22a).[88] Photopolymerization of $Ita3C_{12}$ with methacryl POSS (MAPOSS) cross-linker is used to stabilize the system and improve electro-optical properties. The relative amounts of $Ita3C_{12}$ and MAPOSS are optimized to a molar ratio of 4:1. The theoretical concentration of $Ita3C_{12}$ for forming a monolayer on the LC test cell with a 5 μm cell gap is 0.04 wt%. However, the VA region of the LC test cell appears at this concentration in part. The solubility of $Ita3C_{12}$ in the LC medium is relatively high, and 0.4 wt%, of $Ita3C_{12}$ creates the VA layer in the entire area of the LC test cell (Fig. 22b). Furthermore, the automatically constructed VA layer can be polymerized by irradiating UV light to stabilize the LC alignment layer. After polymerization, the anchoring energy is improved to a level comparable to conventional PI-based alignment. As the concentration of $Itac3C_{12}$ increases, the anchoring energy also increases (Fig. 22c).

To enhance electro-optic properties such as fast response time, low threshold voltage, and wide viewing angle, generating the pre-tilt angle is essential for VA LCDs. The introduced amphiphilic surfactant is migrated to form an automatic VA layer. During the polymerization, the amphiphilic surfactant remaining in the LC medium is polymerized and is completely transferred onto the substrates due to the decrease in solubility.[89] After polymerization under the applied electric field, a pre-tilt angle of 2° is formed (Fig. 23a). As shown in Fig. 23b and 23c, this pre-tilted LC medium significantly enhances electro-optic properties.

6. Discuss and Conclusions

Anisotropic molecular alignment has been extensively used for the display industry. The alignment of the LC molecules is determined by the anisotropic surface energy caused by topology of the substrate as well as the chemical interaction between the LC molecules and the substrate. To induce topologically anisotropic surfaces, the mechanical rubbing has been used. However, the mechanical rubbing method can cause several problems, such as static electricity and optical defects. Direct doping of nanoparticles or giant surfactants in the LC systems can be an ideal candidate to replace the conventional LC alignment. The doped nanoparticles and surfactants in the LC mixture migrate onto the substrate by phase separation and modify the surface to align LC molecules. The automatically fabricated alignment layer induced by doped nanoparticles can be photopolymerized under electric field to align LC molecules with pre-tilt angle for excellent mechanical, electrical and chemical stability with electro-optical high performance.

We have reported and discussed the automatic molecular alignment of the LC molecules by doping of nanoparticles and surfactant to modify interface between LC medium and substrate. The direct doping system can be used to surface modification with anisotropic surficial properties. Furthermore, if most doped nanoparticles are migrated on the substrate and residual doped nanoparticles are remained in bulk of LC medium by controlling solubility of nanoparticle, the LC phase and pretilt angle of LC medium can be precisely handled. This system can allow us to improve technologies of not only electro-optical application but also surface modification.

Conflicts of interest

There are no conflicts to declare.

Acknowledgements

This work was supported by BRL2015042417, MOTIE-KDRC (10051334), Mid-Career Researcher Program (2016R1A2B2011041), NRF Global Ph.D. Fellowship Program of Republic of Korea, and Air Force Office of Scientific Research (FA2386-19-1-4008, USA).

Notes and references

1 M. Schadt, K. Schmitt, V. Kozinkov, and V. Chigrinov, *Jpn. J. Appl. Phys.* 1992, **31**, 2155-2164
2 B. H. Hwang, H. J. Ahn, S. J. Rho, S. S. Chae, and H. K. Baik, *Langmuir*, 2009, **25(14)**, 8306-8312
3 K. Takatoh, M. Hasegawa, M. Koden, N. Itoh, R. Hasegawa, and M. Sakamoto, *Taylor & Francis Inc.: New York*, 2005
4 A. takeda, S. Kataka, T. Sasaki, H. Chida, H. Tsuda, K. Ohmuro, T. Sasabayashi, Y. Koike, and K. Okamoto, *Dig. Tech. Pap.* 2012, **29(1)**, 1077-1080
5 M. Xu, D.-K. Yang, J. Bos, X. Jin, F. W. Harris, and S. Z. D. Cheng, *Dig. Tech. Pap.* 2012, **29(1)**, 139-142
6 S. G. Kim, S. M. Kim, Y. S. Kim, H. K. Lee, and S. H. Lee, *Appl. Phys. Lett.* 2007, **90**, 261910-26192
7 S. H. Lee, S. L. Lee, and H. Y. Kim, *Appl. Phys. Lett.* 1998, **73**, 2881-2883
8 I. H. Yu, I. S. Song, J. Y. Lee, and S. H. Lee, *J. Phys. D: Appl. Phys.* 2006, **39**, 2367-2372
9 P. Kumar, C. Jaggi, V. Sharma, and K. Raina, *Micron* 2016, **81**, 34-47
10 M. Oh-e, and K. Kondo, *Appl. Phys. Lett.* 1996, **69(5)**, 623-625
11 H. Yoshida, and J. R. Kelly, *Jpn. J. Appl. Phys.* 1997, **36**, 2116-2127
12 A. Jakli, *Mol. Cryst. Liq. Cryst.* 1994, **251**, 289-301
13 R. S. Kularatne, H. Kim, J. M. Boothby, and T. H. Ware, *J. Polym. Sci. B. Polym. Phys.* 2017, **55**, 395-411
14 Z. Pei, Y. Yang, Q. Chen, E. M. Terentjev, Y. Wei, and Y. Ji, *Nat. Mater.* 2014, **13**, 36-41
15 L. Zhou, Q. Liu, X. Lv, L. Gao, S. Fang, and H. Yu, *J. Mater. Chem. C* 2016, **4**, 9993
16 Z. Cheng, T. Wang, X. Li, Y. Zhang, and H. Yu, *ACS Appl. Mater. Interfaces* 2015, **7**, 27494-27501
17 H. Yu, *Prog. Polym. Sci.* 2014, **39**, 781-815

18 Z. Cheng, S. Ma, Y. Zhang, S. Huang, Y. Chen, and H. Yu, *Macromolecules* 2017, **50**, 8317-8324
19 D. Zhao, W. Huang, H. Cao, Y. Zheng, C. Wang, Z. Yang, and H. Yang, *J. Phys. Chem. B*, 2009, **113(10)**, 2961-2965
20 B.-Y. Liu, and L.-J. Chen, *J. Phys. Chem. C*, 2013, **117**, 13474-13478
21 J. T. Hunter, S. K. Pal, and N. L. Abbott, *ACS Appl. Mater. Interfaces*, 2010, **2(7)**, 1857-1865
22 M. Yamahara, M. Nakamura, N. Koide, and T. Sasaki, *Liq. Cryst.* 2007, **34(3)**, 381-387
23 J. Stohr, and M. G. Samant, *J. Electron Spectros. Relat. Phenomena*, 1999, **98-99**, 189-207
24 J. H. Kim, M. Yoneya, J. Yamamoto, and H. Yokoyama, *Nanotechnology*, 2002, **13**, 133-137
25 Y. Momoi, O. Sato, T. Koda, A. Nishioka, O. Haba, and K. Yonetake, *Opt. Mater. Express*, 2014, **4(5)**, 1057-1066
26 J. Hoogboom, T. Rasing, A. E. Rowan, and R. J. M. Nolte, *J. Mater. Chem.* 2006, **16**, 1305-1314
27 D. W. Berreman, *J. Chem. Phys.* 1975, **62**, 776-778
28 E. Govers, and G. Vertogen, *Phys. Rev. A*, 1984, **30(4)**, 1998-2000
29 O. A. Rojas-Gomez, and J. M. Romero-Enrique, *Phys. Rev. E*, 2012, **86**, 041706
30 J. M. Geary, J. W. Goodby, A.R. Kmetz, and J. S. Patel, *J. Appl. Phys.* 1987, **62**, 4100-4108
31 D. Dantsker, J. Kumar, and S. K. Tripathy, *J. Appl. Phys.* 2001, **89**, 4318-4325
32 J. R. Dennis, and V. Vogel, *J. Appl. Phys.* 1998, **83**, 5195-5202
33 W. M. Gibbons, P. J. Shannon, S.-T. Sun, and B. J. Swetlin, *Nature* 1991, **351**, 49-50
34 Y. S. Negi, I. Kawamura, and Y. Suzuki, N. Yamamoto, Y. Yamada, M. Kakimoto, and Y. Imai, *Mol. Cryst. Liq. Cryst.* 1994, **239**, 11-25
35 H. Yaning, L. Bin, R. Hongfeng, and W. Xiaogong, *Front. Chem. China* 2007, **2(3)**, 318-321
36 H. Kang, J. S. Park, E.-H. Sohn, D. Kang, C. Rosenblatt, and J.-C Lee, *Polymer* 2009, **50**, 5220-5227
37 F. Wang, L. Shao, Q. Bai, X. Che, B. Liu, and Y. Wang, *Polymers* 2017, **9**, 233
38 Z. Liu, F. Yu, Q. Zhang, Y. Zeng, and Y. Wang, *Eur. Polym. J.* 2008, **44**, 2718-2727
39 W.-Y. Wu, C.-C. Wang, and A. Y.-G. Fuh, *Opt. Express* 2008, **16(21)**, 17131-17137
40 J.-H. Lee, Y. E. Choi, J. H. Lee, B. H. Lee, W. I. Song, K.-U. Jeong, G.-D. Lee, and S. H. Lee, *J. Phys. D: Appl. Phys.* 2013, **46**, 485503
41 S. W. Lee, S. I. Kim, Y. H. Park, M. Ree, Y. N. Rim, H. J. Yoon, H. C. Kim, and Y. B. Kim, *Mol. Cryst. and Liq. Cryst.* 2000, **349**, 279-282
42 Y. Tsuda, J. M. Oh, and R. Kuwahara, *Int. J. Mol. Sci.* 2009, **10**, 5031-5053
43 H. Kang, J.-H. Lee, D.-G. Kim, and D. Kang, *Mol, Cryst. Liq. Cryst.* 2015, **607**, 94-103
44 S. H. Lee, S. S. Bhattacharyya, H. S. Jin, and K.-U. Jeong, *J. Mater. Chem.* 2012, **22**, 11893-11903
45 A. Rastegar, M. Skarabot, B. Blij, and Th. Rasing, *J. Appl. Phys.* 2001, **89**, 960-964
46 M. Behdani, A. Rastegar, S. H. Keshmiri, S. I. Missat, E. Vlieg, and Th. Rasing, *Appl. Phys. Lett* 2002, **80**, 4635-4637
47 C.-Y. Lee, Y.-W. Li, M.-C. Tseng, V. G. Chigrinov, and H.-S. Kwok, *J. Soc. Inf. Disp.* 2015, **23(5)**, 202-213
48 P. Kumar, S. Y. Oh, V. K. Baliyan, S. Kundu, S. H. Lee, and S.-W. Kang, *Opts. Express* 2018, **26(7)**, 8385-8396
49 H. S. Jeong, H.-J. Jeon, Y. H. Kim, M. B. Oh, P. Kumar, S.-W. Kang, and H.-T. Jung, *NPG Asia Mater.* 2012, **4**, e7
50 R. Lin, and J. A. Rogers, *Nano Lett.* 2007, **7(6)**, 1613-1621
51 P. Im, Y.-J. Choi, W.-J. Yoon, D.-G. Kang, M. Park, D.-Y. Kim, C.-R. Lee, S. Yang, J.-H. Lee, and K.-U. Jeong, *Sci. Rep.* 2016, **6**, 36472
52 J. Sun, R. Lan, Y. Gao, M. Wang, W. Zhang, L. Wang, L. Zhang, Z. Yang, and H. Yang, *Adv. Sci.* 2018, **5**, 1700613
53 J. Sun, L. Yu, L. Wang, C. Li, Z. Yang, W. He, C. Zhang, L. Zhang, J. Xiao, X. Yuan, F. Li, and H. Yang, *J. Mater. Chem. C* 2017, **5**, 3678-3683
54 V. Chigrinov, E. Prudnikova, V. Kozenkov, Z. Ling, and H. S. Kwok, *Dig. Tech. Pap.* 2012, **33(1)**, 1106-1109
55 V. Chigrinov, A. Muravski, and H. S. Kwok, *Phys. Rev. E* 2003, **68**, 061702
56 T. Seki, *Polym. J.* 2014, **46**, 751-768
57 K. Beppu, Y. Nagashima, M. Hara, S. Nagano, and T. Seki, *Macromol. Rapid Commun.* 2017, **38**, 1600659
58 G. Hegde, R. A. Alla, A. Matharu, and L. Komitov, *J. Mater. Chem. C* 2013, **1**, 3600-3605
59 A. Bobrovsky, A. Ryabchum, and V. Shibaev, *J. Photochem. Photobiol. A: Chem.* 2011, **218**, 137-142
60 D. D. Huang, E. P. Pozhidaev, V. G. Chigrinov, H. L. Cheung, Y. L. Ho, and H. S. Kwok, *Displays* 2004, **25**, 21-29
61 M. Sano, M. Hara, S. Nagano, Y. Shinohara, Y. Amemiya, and T. Seki, *Macromolecules* 2015, **48**, 2217-2223
62 H. Yu, T. Iyoda, and T. Ikeda, *J. Am. Chem. Soc.* 2006, **128**, 11010-11011
63 H. Yu, and T. Ikeda, *Adv. Mater.* 2011, **23**, 2149-2180
64 O. Yaroshchuk, and Y. Reznikov, *J. Mater. Chem.* 2012, **22**, 286-300
65 K. Ichimura, *Chem. Rev.* 2000, **100**, 1847-1873
66 M. Nishikawa, B. Taheri, and J. L. West, *Appl. Phys. Lett.* 1998, **72(19)**, 2403-2405
67 B.-N. Yang, and D.-M. Shin, *Mol, Cryst. Liq. Cryst.* 2014, **599**, 118-124
68 O. Haba, D. Hiratsuka, T. Shiraiwa, N. Funakoshi, H. Awano, T. Koda, T. Takahashi, K. Yonetake, M. Kwak, Y. Momoi, N. Kim, S. Hong, D. Kang, and Y. Choi, *Opts. Mater. Express* 2014, **4(5)**, 934-943
69 K.-H. Kim, B. W. Park, S.-W. Choi, J.-H. Lee, H. Kim, K.-C. Shin, H. S. Kim, and T.-H. Yoon, *Liq. Cryst.* 2013, **40(3)**, 391-395
70 P. S. Noonan, A. Shavit, B. R. Acharya, and D. K. Schwartz, *ACS Appl. Mater. Interfaces* 2011, **3**, 4374-4380
71 S.-H. Lee, J.-H. Son, W.-C.Zin, S. H. Lee, and J.-K. Song, *Liq. Cryst.* 2012, **39(9)**, 1049-1053
72 S.-J. Hwang, S.-C. Jeng, C.-Y. Yang, C.-W. Kuo, and C.-C. Liao, *J. Phys. D: Appl. Phys.* 2009, **42**, 025102
73 S.-C. Jeng, C.-W. Kuo, H.-L. Wang, and C.-C. Liao, *Appl. Phys. Lett.* 2007, **91**, 061112
74 S.-H. Chen, T.-R. Chou, Y.-T. Chiang, and C.-Y. Chao, *Molecular crystals and liquid crystals* 2017, **646**, 107-115
75 S.-J. Hwang, Y.-M. Shieh, and K.-R. Lin, J. *Nanomaterials* 2015, **2015**, 840182
76 H. Qi, and T. Hegmann, *J. Mater. Chem.* 2008, **18**, 3288-3294
77 S. Kumar, S. K. Pal, P. S. Kumar, and V. Lakshminarayanan, *Soft Matter* 2007, **3**, 896-900
78 J. W. Goodby, I. M. Saez, S. J. Cowling, V. Gortz, M. Draper, A. W. Hall, S. Sia, G. Cosquer, S.-E. Lee, and E. P. Raynes, *Angew. Chem. Int. Ed.* 2008, **47**, 2754-2787
79 X. Yu, K. Yue, I-F. Hsieh, Y. Li, X.-H. Dong, C. Liu, Y. Xin, H.-F. Wang, A.-C. Shi, G. R. Newkome, R.-M. Ho, E.-Q. Chen, W.-B. Zhang, and S. Z. D. Cheng, *PNAS* 2013, **110(25)**, 10078-10083
80 A. Patra, Ch. G. Chandaluri, and T. P. Radhakrishnan, *Nanoscale* 2012, **4**, 343-359
81 Y. Li, W.-B. Zhang, I-F. Hsieh, G. Zhang, Y. Cao, X. Li, C. Wesdemiotis, B. Lotz, H. Xiong, and S. Z. D. Cheng, *J. Am. Chem. Soc.* 2011, **133**, 10712-10715
82 D.-Y. Kim, S.-A Lee, S. Kim, C. Nah, S. H. Lee, and K.-U. Jeong, *Small* 2018, **14**, 1702439

83 H. Qi, and T. Hegmann, *ACS Appl. Mater. Interfaces* 2009, **1(8)**, 1731-1738
84 D.-Y. Kim, S. Kim, S.-A. Lee, Y.-E. Choi, W.-J. Yoon, S.-W. Kuo, C.-H. Hsu, M. Huang, S. H. Lee, and K.-U. Jeong, *J. Phys. Chem.* 2014, **118**, 6300-6306
85 I. Son, J. H. Kim, B. Lee, C. Kim, J. Y. Yoo, K. Hyun, J.-P. Wu, and H. Lee, *Marcomol. Res.* 2016, **24(3)**, 235-239
86 D.-Y. Kim, S.-A Lee, D.-G. Kang, M. Park, Y.-J. Choi, and K.-U. Jeong, *ACS Appl. Mater. Interfaces* 2015, **7**, 6195-6204
87 D.-Y. Kim, S.-A Lee, M. Park, and K.-U. Jeong, *Chem. Eur. J.* 2015, **21**, 545-548
88 W.-J. Yoon, Y.-J. Choi, D.-Y. Kim, J. S. Kim, Y.-T. Yu, H. Lee, J.-H. Lee, and K.-U. Jeong, *Macromolecules* 2016, **49**, 23-29
89 W.-J. Yoon, Y.-J. Choi, D.-G. Kang, D.-Y. Kim, M. Park, J.-H. Lee, S.-W. Kang, S. H. Lee, and K.-U. Jeong, *ACS Omega* 2017, **2**, 5942-5948
90 J. Stohr, M. G. Samant, J. Luning, A. C. Callegari, P. Chaudhari, J. P. Doyle, J. A. Lacey, S. A. Lien, S. Purushothaman, and J. L. Speidell, *Science* 2011, **292**, 2299-2302
91 S. G. Hahm, T. J. Lee, T. Chang, J. C. Jung, W.-C. Zin, and M. Ree, *Macromolecules* 2006, **39**, 5385-5392
92 R. Basu, and S. A. Shalov, *Phys. Rev. E* 2017, **96**, 012702
93 X. Li, Y. Zhu, W. Cai, M. Borysiak, B. Han, D. Chen, R. D. Piner, L. Colombo, and R. S. Ruoff, *Nano Lett.* 2009, **9(12)**, 4359-4363
94 X. Liang, B. A. Sperling, I. Calizo, G. Cheng, C. A. Hacker, Q. Zhang, Y. Obeng, K. Yan, H. Peng, Q. Li, X. Zhu, H. Yuan, A. R. H. Walker, Z. Liu, L. Peng, and C. A. Richter, *ACS Nano* 2011, **5(11)**, 9144-9153
95 H. Chen, Y. Weng, D. Xu, N. V. Tabiryan, and S.-T. Wu, *Opt. Express* 2016, **24(7)**, 7287-7298
96 S.-K. Park, S.-E. Kim, D.-Y. Kim, S.-W. Kang, S. Shin, S.-W. Kuo, S.-H. Hwang, S. H. Lee, M.-H. Lee, and K.-U. Jeong, *Adv. Funct. Mater.* 2011, **21**, 2129-2139
97 Y.-J. Bae, H.-J. Yang, S.-H. Shin, K.-U. Jeong, and M.-H. Lee, *J. Mater. Chem.* 2011, **21**, 2073-2077
98 P. Im, D.-G. Kang, D.-Y. Kim, Y.-J. Choi, W.-J. Yoon, M.-H. Lee, I.-H. Lee, C.-R. Lee, and K.-U. Jeong, *ACS Appl. Mater. Interfaces* 2016, **8**, 762-771
99 S.-R. Yoon, H.-J. Yang, K.-U. Jeong, and M.-H. Lee, *Jpn. J. Appl. Phys.* 2013, **52**, 05DB12
100 J. I. Uy, C. L. Asbury, T. W. Petersen, and G. Engh, *Cytometry A* 2004, **61**, 18-25
101 M. Nakata, G. Zanchetta, M. Buscaglia, T. Bellini, and N. A. Clark, *Langmuir* 2008, **24**, 10390-10394
102 D.-R. Chiou, and L.-J. Chen, *Langmuir* 2006, **22**, 9403-9408
103 C.-J. Hsu, B.-L. Chen, and C.-Y. Huang, *Opt. Express* 2016, **24(2)**, 1463-1471
104 A. Choudhary, T. F. George, and G. Li, *Cornell University Library* 2015
105 S. Orlandi, E. Benini, I. Miglioli, D. Evans, V. Reshetnyak, and C. Zannoni, *Phys. Chem. Chem. Phys.* 2016, **18**, 2428-2441
106 J. Cognard, *Mol. Cryst. Liq. Cryst.* 1982, **1**, 1-78
107 B. Liu, Y. Ma, D. Zhao, L. Xu, F. Liu, W. Zhou, and L. Guo, *Nano Res.* 2017, **10**, 618-625
108 W. Zhou, L. Lin, D. Zhao, and L. Guo, *J. Am. Chem. Soc.* 2011, **133**, 8389-8391
109 D. Zhao, W. Zhou, X. Cui, Y. Tian, L. Guo, and H. Yang, *Adv. Mater.* 2011, **23**, 5779-5784
110 S. Kundu, M.-H. Lee, S. H. Lee, and S.-W. Kang, *Adv. Mater.* 2013, **25**, 3365-3370
111 R. He, P. Wen, S.-W. Kang, S. H. Lee, M.-H. Lee, *Liq. Cryst.* 2018, **45(9)**, 1-11

Table of Content (ToC) of

"Giant Surfactants for the Construction of Automatic Liquid Crystal Alignment Layers"

Won-Jin Yoon,
Kyung Min Lee,
Dean R. Evans,
Michael E. McConney,
Dae-Yoon Kim,
Kwang-Un Jeong*

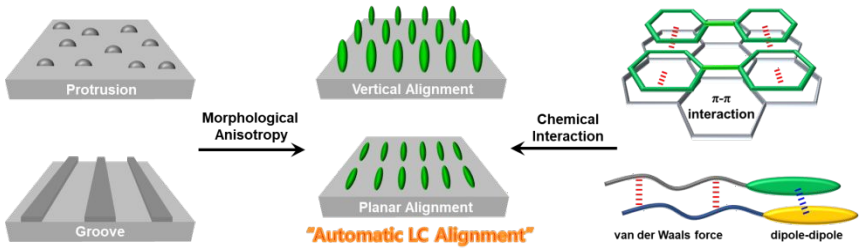

Liquid crystal molecules were automatically aligned by not only morphological anisotropy but also chemical interaction.